Ultrastructure of Ectopic Peritoneal Lesions From Women With Endometriosis, Including Observations on the Contribution of Coelomic Mesothelium

Carolyn J. P. Jones, PhD, **Luciano G. Nardo, MD**, **Pietro Litta, MD**, and **Asgerally T. Fazleabas, PhD**

From the Maternal and Fetal Health Research Centre, School of Clinical and Laboratory Science, University of Manchester, St Mary's Hospital, Manchester, United Kingdom (CJPJ, LGN); Department of Reproductive Medicine, St Mary's Hospital, Manchester, United Kingdom (LGN); Department of Obstetrics and Gynaecology, University of Padua, Padua, Italy (PL); and Center for Women's Health and Reproduction, Department of Obstetrics and Gynecology, University of Illinois at Chicago, Chicago, Illinois (ATF)

Abstract

Following a study in a baboon model of endometriosis, we here describe the morphology of ectopic peritoneal lesions in the human to examine the effects of an ectopic site on glandular structure and function. Ectopic biopsies from 17 women with endometriosis were fixed and processed for electron microscopy. Certain biopsies were also probed for intermediate filaments using immunohistochemistry. Ultrastructurally, lesions showed many different glandular morphologies with indications of delayed maturation compared to normal endometrium. Mesothelium covered some lesions and there was evidence of mesothelial invasion into the stroma. Ectopic endometriotic lesions from women with endometriosis showed ultrastructural differences from eutopic endometrium, with indications that mesothelial invasion may contribute to gland development in some lesions.

Keywords

Endometriosis; ultrastructure; human; coelomic mesothelium

INTRODUCTION

Endometriosis is defined as the presence of endometrial glands and stroma outside the uterine cavity, usually found over peritoneal and visceral surfaces within the pelvis. It is one of the most common causes of infertility and chronic pelvic pain, affecting about 1 in 10 women in the reproductive-age group.[1] This incidence increases up to 30% in patients with infertility and up to 45% in patients with chronic pelvic pain.[2] Although existence of this disease has been known for over a century, there is still much controversy over the fundamental mechanisms by which menstrual endometrium adheres to, proliferates and establishes a functional vasculature in an ectopic site. The "implantation" theory of endometriosis suggests that retrograde menstruation is the source of endometriotic lesions[3] while in the alternative "metaplastic" theory it is proposed that a factor in the menstrual debris induces metaplasia of the mesothelial lining cells.[4]

Address correspondence to: Carolyn J. P. Jones, PhD, Department of Obstetrics and Gynaecology, University of Manchester, St Mary's Hospital, Hathersage Road, Manchester M13 0JH, United Kingdom. E-mail: carolyn.jones@manchester.ac.uk.

In this study, we are extending our observations from a baboon model of endometriosis[5] to biopsies from ectopic, peritoneal sites obtained from women with visually and histologically proven endometriosis, examining the ultrastructure of the tissues to further our understanding of the pathobiology of this disease.

MATERIALS AND METHODS

Study Population

The study group comprised 17 women with visually and biopsy-proven endometriosis who had undergone laparoscopic excision of endometriotic deposits and endometrial curettage. All women with endometriosis complained of pelvic pain, deep dyspareunia, and/or sub-fertility. None of the participants had an intrauterine device in situ or had received hormonal therapy in the 3 months preceding laparoscopy and endometrial sampling. Endometriosis at the time of laparoscopy was staged according to the revised American Fertility Society (rAFS) scoring system.[6] Some of the specimens in the sample were lacking glands (Table 1) due to the bulk of the specimen being sent for histopathological examination for diagnostic purposes but had a surface covering of mesothelium which was examined for ultrastructural changes.

The study was approved by the local research ethics committee (Ref Number 06/Q1407/173) as well as by the Universities of Manchester, United Kingdom, and Padua, Italy. All women gave written informed consent to participate in the study.

Tissue

Tissues (Table 1) were obtained from the Department of Obstetrics and Gynaecology, University of Padua, Italy. All chemicals and reagents were obtained from Sigma (United Kingdom or Italy) unless otherwise specified. Tissue was fixed in half-strength Karnovsky fixative [2% w/v paraformaldehyde and 2.5% glutaraldehyde (v/v) in 0.1 M phosphate buffer pH 7.2] for 24 to 48 hours then rinsed in buffer and transported to the United Kingdom. Tissues were diced into 1-mm thick slices before further processing, postfixed in 1% osmium tetroxide (Agar Scientific Ltd, Stansted, United Kingdom)/1.5% potassium ferrocyanide in 0.05 M sodium cacodylate buffer pH 7.2 for 1 hour in the dark, rinsed twice in buffer, dehydrated, and processed into Taab epoxy resin (TAAB Laboratories Equipment Ltd, Aldermaston, United Kingdom) for electron microscopy. Semithin 0.5-μm sections were cut on a Reichert Ultracut microtome using a diamond knife, stained with 1% toluidine blue in 1% borax on a hotplate, and suitable areas containing glands and/or surface epithelium selected for further examination.

Electron Microscopy

Ultrathin sections of the osmicated material, 70-nm thick, were mounted on 200 mesh copper grids and contrasted with uranyl acetate (Agar Scientific Ltd)/lead citrate and examined in a Philips CM-10. Digital images were captured using a Deben camera and stored as 4MB TIFF files.

Immunocytochemistry

About 2 endometriotic specimens that showed features of mesothelial cell invasion were examined using immunohistochemistry. Sections were cut and dried as for lectin histochemistry[5] and were treated in a similar manner with respect to removal of resin and blocking of endogenous peroxidase activity. Antigen retrieval was carried out by microwaving in 0.01 M citrate buffer pH 6.0 for 2 periods of 5 minutes each followed by 20 minutes cooling at room temperature. Sections were rinsed in water then 0.05 M Tris buffered saline (TBS). Treatment with blocking serum (0.1% Tween, 10% normal rabbit serum, 2% normal human serum in 0.3M NaCl high salt buffer) for 20 minutes was followed by incubation in the primary

antibodies [monoclonal mouse anti-human Cytokeratin 7 (Dako, Ely, United Kingdom) 1:200; monoclonal mouse anti-human Pancytokeratin (Dako) 1:200, 1:400; monoclonal mouse anti-CD 34 (Serotec, Oxford, United Kingdom) 1:1000; monoclonal mouse anti-vimentin (Novocastra, Newcastle-Upon-Type, United Kingdom) 1:100] overnight at 4°C in a humidity chamber. After washing in TBS, biotinylated goat antimouse (1:200) secondary antiserum (Dako) was applied for 1 hr at 37°C. Sections were washed in TBS then the avidin-peroxidase/ DAB revealing system used as for lectin histochemistry[5], with a similar counterstain.

RESULTS

Electron Microscopy

The most striking aspect of the ultrastructure of endometriotic lesions was their heterogeneity and their various features have been summarized in Table 2. The outer mesothelium was generally fairly uniform in its ultrastructure (Table 3) but glands and cystic structures varied greatly in their morphology and bore little relationship to their eutopic equivalents as described in the literature with respect to their position in the menstrual cycle. A biopsy taken on day 9 (PL003) most resembled eutopic endometrium in that gland cells were columnar with euchromatic, regularly shaped nuclei, and a normal distribution of organelles (Figure 1A), though one distinctive feature not seen in eutopic endometrium was the presence of large basal vacuoles filled with amorphous material. The apices of the cells were covered with microvilli borne on protuberances and an occasional mitotic figure could be seen (Figure 1B). Scattered foci of glycogen were present and occasional secretory droplets. Sparsely distributed profiles of pale cells with electron lucent cytoplasm and whorls of endoplasmic reticulum were evident between the columnar cells, as well as occasional lymphocytes (Figure 1C). In other areas, there were infoldings from the surface mesothelium dipping down to form gland-like structures with morphology intermediate between flattened surface mesothelial cells and cuboidal epithelium (Figure 1D).

These pale cells were also present in 3 biopsies taken on days 15 (PL001) and 17 (PL005, PL021) and in places were a prominent feature (Figures 1D and 2A). They were characterized by concentric cisternae of endoplasmic reticulum, small mitochondria, and euchromatic nuclei with some peripheral heterochromatin, and lacked desmosomal contacts with their neighbors. They occupied intercellular spaces that were filled with flocculent material (Figure 1E) and also appeared loose in the stroma forming nests or aggregates of cells, sometimes associated with mitotic figures (Figure 1F). In one day 17 case (PL005), tubular or gland-like structures were also found in the stroma (Figure 1G), the cells here being joined together with desmosomes and apical tight junctions (Figure 1H).

The gland cells associated with areas of pale cell migration were generally columnar, sometimes with apical structures resembling pinopodes, having smooth surfaces and being devoid of organelles (Figure 2A); in PL001 (day 15), there were some flattened cells forming arcades over the large intercellular spaces filled with flocculent material (Figure 1E). Nuclei were euchromatic with large, complex nucleoli and narrow cisternae of endoplasmic reticulum coursed through the cells, with small mitochondria, collapsed Golgi saccules and occasional secretory droplets. In one day 17 specimen (PL005), there were significant aggregates of glycogen, a feature not observed in other cases (Figure 2B). The cells lining the glands and cysts usually bore slender microvilli on their apices except where pinopodes were present; there were occasional ciliated cells and intraepithelial lymphocytes. Pale cells with large heterolysosomes were also found in one of the day 15 epithelium (PL001), with narrow cisternae of endoplasmic reticulum (Figure 2C).

There was also some heterogeneity in the nature of the glycocalyx covering the microvilli. This was generally inconspicuous, but one case (day 17, PL021) had an extremely electron-dense

layer on one area of cells lining a cyst (Figure 2D); this took the form of evenly spaced filaments extending from the microvilli and was a highly unusual feature. These cells did not contain an excessive number of secretory droplets although stacks of Golgi saccules were present.

Most of the other lesions contained glands or cystic structures that were lined by cuboidal cells and these ranged from days 15 to 27 of the cycle, though a fibrous, fatty lesion (PL031, day 21) containing a large cyst filled with fatty, degenerative material was lined by cells which were extremely flat and attenuated, with very heterochromatic nuclei and few identifiable organelles (Figure 2E). Surrounding tissues were also fibrous and fatty. In general, however, nuclei were euchromatic, in some cases (day 15, PL017, day 17 PL021, 027) heavily incised to produce a highly irregular, lobulated profile (Figure 2F). Mitochondria were generally small and round and dispersed through the cell with short strands of rough endoplasmic reticulum. Golgi saccules were usually inconspicuous with few secretory droplets and finely dispersed rosettes of glycogen may be present. Ciliated cells were often present, being electron-lucent with a distinctive morphology. In one case (day 22, PL024), however they were seen in a small cyst and had a somewhat unusual ultrastructure, the cilia being admixed with microvilli and closely packed and straight; at the light microscope level, they could be seen sticking straight out into the lumen-like bristles or spikes (Figure 2G). The cells lining this cyst were highly polarized, containing supranuclear clusters of fatty inclusions and were packed with mitochondria both basally and apically. Cisternae of rough endoplasmic reticulum were also quite prominent in places and lateral membranes interdigitated closely basally. The lumen of the cyst contained flocculent, amorphous material which coated the cilia and microvilli.

Despite the occurrence of hemorrhage associated with endometriotic lesions, only one case (day 27, PL022) showed evidence of heterolysosomes containing material of moderate electron density (possibly hemosiderin, Figure 3A). These were often present as giant inclusions of a heterogeneous nature and almost all of the epithelial cells, both ciliated and microvillous, contained similar material in greater or smaller amounts. Another feature of these cells was the presence of complex basal infoldings of the cell membranes (Figure 3B).

In spite of the heterogeneous nature of the lesions and component cells, there were certain features common to all the biopsies. These were a notable dearth of glycogen accumulation in the second part of the cycle, apart from isolated aggregates seen in one day 17 biopsy (PL005) (Figure 2B) and absence of both giant mitochondria (normally found between days 15 and 19) and nucleolar channel systems (characteristic of days 17–20). Nucleoli were, however, very large and complex in most of the specimens, with a very elaborate ultrastructure. Gland ultrastructure was nevertheless very variable between lesions, even those obtained on similar days of the cycle (Figures 1E and 2F), as well as within the same lesion (Figures 1A and 1D).

Many of the lesions containing cysts and glands were covered with a layer of flattened or scalloped cells, probably mesothelial in origin, as were specimens devoid of glands [days 5, 8, 13, 20, 21 (1 specimen), 24 (1 specimen), 25, and 29]. The characteristics of these cells have been summarized in Table 3 and they invariably contained heterochromatic, irregularly shaped nuclei and sparse organelles. Large intercellular spaces filled with flocculent material were sometimes present. In one case (day 13, PL006), there was an invagination of the scalloped surface cells to form a gland-like structure with amorphous material in the lumen (Figure 3C). A necrotic area was present on a day 25 lesion. Although no true glands were evident in a day 20 specimen (PL023), a nest of cells was found in the stroma, with incised, heterochromatic nuclei and large nucleoli, and desmosomal contacts between cells (Figure 3D). Part of the lining cells of lesions taken on days 20 and 29 showed greatly enlarged, columnar or tongue-like cells as opposed to the flattened phenotype (Figure 3E). Secretory apparatus such as Golgi saccules and cisternae of endoplasmic reticulum were particularly well developed in these cells (PL023), and occasional small aggregations of glycogen were also present (Figure 3F). A feature of

particular interest was observed in semithin sections in one of the cystic day 17 specimens (PL005) which had pale cells at the ultrastructural level, transitions between flattened and columnar cells could be seen on the surface (see section on immunocytochemistry) and also on a lesion from day 24 (PL026) which contained a cyst but also had areas with tongue-like cells lining grooves dipping in to the lesion from the surface, suggesting the local development of a columnar phenotype.

Immunohistochemistry

Cytokeratin 7 was found to stain a subpopulation of mesothelial cells on the surface of an ectopic lesion (PL005) as well as cells forming a network of glandular structures in the stroma (Figures 4A and B). This specimen had shown evidence of new growth of glandular structures and nests of cells at the electron microscope level. Most of the surface epithelium and the glands composed of columnar epithelium were unstained with this antibody (Figures 4A-C). Some of the mesothelial cells also expressed low levels of vimentin (Figure 4D), as did stromal cells, though the surface nucleolar epithelium and glandular structures did not (Figures 4D and E). Another specimen (PL001) with a large cystic gland showed an area of vimentin-positive flattened cells abutting the lumen, with occasional intraepithelial cells that were also vimentin positive (Figure 4F). Staining with anti-CD34 identified capillaries while the cytokeratin-positive cells remained unstained (not shown).

DISCUSSION

Ultrastructural examination of peritoneal endometriotic lesions revealed significant differences from the reported descriptions of eutopic endometrium[7–11] as well as morphological heterogeneity, with a wide range of appearances between similarly dated specimens. This implies heterogeneity in the presence of local factors around the lesions which may influence their development and differentiation. A major feature was an apparent failure in normal endometrial differentiation, for although the earliest ectopic lesion with glandular structures (day 9) showed a similar ultrastructure to that of normal eutopic epithelium, apart from the presence of some large intracytoplasmic vacuoles, most later specimens exhibited a much earlier phenotype than would be expected for the phase in the cycle. Nuclei were euchromatic and, apart from one case with some aggregates, the cytoplasm contained very little glycogen which normally accumulates basally in the early secretory phase of the cycle. The presence of glycogen in eutopic endometrium is vital for the production of secretions for the nourishment of an implanting blastocyst and its absence in ectopic lesions is one of the most important functional differences between eutopic and ectopic endometrium. The lack of glycogen, endoplasmic reticulum, and mitochondrial morphology was more like that associated with the proliferative phase of the cycle and may reflect the reported increased oestrogen concentrations in endometriotic lesions.[12]

Other features signifying failure of differentiation that were common to all the biopsies examined were the lack of nucleolar channel systems and giant mitochondria which are normally found in the early secretory phase. In some cases, the nucleoli appeared very complex and it is possible that some components of the channel system were being synthesized but not assembled appropriately. Previous ultrastructural studies on endometriotic implants also reported the absence of these features[13–15] and noted delayed maturation in many cases. Experimental evidence has suggested that the development of the nuclear channel system is a response to the acyl group in the 17-β position of the D-ring of progestational steroids, and endometrial adenocarcinomas exposed to medroxyprogesterone acetate developed this structure.[16] This may also be associated with increased progesterone resistance in these tissues[17]; lack of progesterone receptors may prevent the intracellular signaling necessary for the biosynthesis of these structures. Extremely incised nuclei were also seen in some cells

lining the cysts and in the mesothelial cells around the lesions in many cases, a feature associated with heightened metabolic activity often seen in tumors[18] and may reflect abnormalities of growth in these tissues.

With respect to the pale cells that were observed in several cases, similar cells have been described before in ectopic lesions[14] but their possible significance was perhaps not fully appreciated. Pale cells have been seen by us in very early (day 4) glands from eutopic endometrium (unpublished data) which suggests that they might be involved in normal glandular regeneration. Their euchromatic nuclei differed from those of the occasional intraepithelial lymphocytes but, like these, they did not appear to have attachments to neighboring cells. Some of these cells contained large phagosomes and/or concentric cisternae of endoplasmic reticulum; the phagosomes suggested that they were macrophages but the presence of the cisternae of endoplasmic reticulum argued against this. Schweppe and co-workers[15] also observed cells containing phagosomes.

In several ectopic lesions examined by us, there were areas where these undifferentiated pale cells seemed to be in transit between the epithelium and stroma. They appeared to derive from epithelium, but their origin was not always clear; the possibility remains that some of them, at least, could be activated leukocytes. Others made connections with similar cells in the stroma to form cell nests which may have been precursors of the simple tubules with desmosomal contacts which were evident in a day 17 lesion. Whether these primitive glandular structures were derived from mesothelium or from endometrial glands was not always evident at the ultrastructural level. However, our preliminary immunocytochemical data support the suggestion that some invasive cells are derived from the mesothelium, as they express cytokeratin-7 which is not found in the glandular endometriotic cells under our conditions of fixation and resin embedding. Cytokeratin-7 is a neutral-basic class B (type II) subfamily of cytokeratins can be used to recognize specific subtypes of adenocarcinoma[19,20] and has been shown to be positive in 97% of endometrioid tumors.[21] Newly formed, tubular structures that expressed cytokeratin-7 were clearly a part of a mesothelial reaction, but cystic/glandular structures with a more cuboidal epithelium, or those with large intercellular spaces, were not easy to classify. There have been reports of surface peritoneal/mesothelial cells dipping into the stroma of ectopic lesions and forming glandular structures[22] as in the day 17 ectopic specimen seen here.

Immunocytochemical studies[23] have shown that, in endometriosis, some mesothelial cells adjacent to endometriotic lesions can also take on the characteristics of epithelium such as binding by Ber-EP4 antibody, thus implying that mesothelial cells may undergo epithelial differentiation and alter their marker status. We observed that surface cells in a day 17 (PL005) specimen varied between a flattened and columnar phenotype and have shown the presence of vimentin-positive cells adjacent to vimentin-negative epithelium in a lesion, suggesting a possible relationship between the two.

Mesothelial cells have been shown to share characteristics of both epithelial and mesenchymal cell types and range from flattened to cuboidal in shape, depending on their site in the body and state of activation.[24] Mesothelial cells found on the surface of some lesions were similar to the flattened and cuboidal cells described by Schweppe[13] and Schweppe and colleagues[15] in their study of endometriotic tissue, and similar cells were seen here lining some of the cysts.

The coelomic metaplasia theory concerning the etiopathogenesis of endometriosis of the peritoneum proposes that mesothelial cells on the ovary or pelvis are serially changed to endometriotic gland cells.[4,25,26] Mesothelial inclusions have been found to be associated with endometriosis in ovaries, fallopian tube, and pelvic wall[27] and in one case continuity was

shown between the surface epithelium and mesothelial inclusions, as in our study. Kerner and colleagues[27] described nests of cells, of surface mesothelial origin, often without or with a barely discernable lumen. In vitro studies[28] have also shown that surface ovarian mesothelium cultured with endometrial stromal cells in a 3-dimensional collagen gel lattice can form glandular structures with a lumen, with immunoreactivity for cytokeratin and epithelial membrane antigen. Component cells were in contact via tight junctions, much as we have seen here.

As well as mesothelium, fragments of endometrium are capable both of invading a matrix culture system and forming tubular structures[29]; they can attach and adhere to the peritoneum and undergo transmesothelial invasion.[30,31] Our initial immunocytochemistry indicates, however, that endometrial-type epithelium is probably not involved in the process of tubule formation by pale cells observed in our lesions. It is therefore possible that the contribution of mesothelial cells to the growth and development of endometriotic lesions is not yet fully appreciated.

Previous studies have reported the existence of an invasive, N-cadherin-expressing epithelial cell type in endometriosis[32,33] as opposed to the columnar E-cadherin-positive cells which are terminally differentiated and polarized. Pilot studies (not shown) attempting to identify E-cadherins and N-cadherins in our plastic tissue sections were unsuccessful due to the presence of glutaraldehyde in the fixative, which cross-links proteins, but it is possible that the invasive pale cell that we observed might have been analogous to the N-cadherin-expressing cells described by other authors. However, in the baboon model of endometriosis, E-cadherin is not present in the ectopic lesions.[34]

The lack of differentiation in the cells lining the cysts may indicate a mesothelial origin of some glands as well as progesterone resistance, together with a deficiency in 17-β-hydroxysteroid dehydrogenase type 2 in glandular epithelial cells.[35,36] Aromatase activity, not usually found in endometrium, and which catalyzes the conversion of C19 steroids to estrogens, has also been described in endometriotic lesions.[12,37,38] This enzyme-driven increase in endogenous oestrogen biosynthesis is thought to be one of the factors that sustain the endometriotic lesions, partially or totally mediated by estrogen receptor-α positive stromal cells[39] present in red peritoneal lesions.[40] This is also possibly associated with a concomitant lack of progesterone receptor B and low levels of progesterone receptor A in endometriotic tissue,[22] though some studies have found levels of such receptors to be high.[41] These findings have been reviewed by Nisolle and Donnez[42] who concluded that the persistence of progesterone receptors in both epithelium and stroma of endometriotic lesions may explain the inefficacy of medical therapy. The relationship between epithelial columnar cells and adjacent mesothelium has also been discussed with reference to the presence of estrogen and progesterone receptors in epithelial and stromal cells.[43]

In conclusion, our study has demonstrated significant heterogeneity and abnormalities in the tissue architecture of ectopic lesions compared to eutopic endometrium. Ultrastructural and immunocytochemical evidence also points toward an important contribution of the mesothelium to growth of ectopic structures. Plastic embedded material is not ideal for immunohistochemical studies and our original aims did not include this aspect of the work. It is notoriously difficult to undertake immunocytochemistry on glutaraldehyde-fixed, plastic-embedded material due to the extreme cross-linking of proteins that occurs and the prolonged fixation of the tissues (24–48 hours) would exacerbate this. The negative results obtained with many of the antibodies may be explained by these factors, though the lack of stain was, in some instances—for example, the limited cytokeratin-7 expression—useful in differentiating the various cell types that occurred in the lesions. Further studies are now in progress using appropriately fixed and embedded tissue to localize steroid receptors in paired ectopic and

eutopic tissues and to characterize the cells with invasive phenotypes that appear in these lesions. This may enhance our understanding of the different clinical entities of endometriosis —peritoneal, ovarian, and rectovaginal—and perhaps explain the biological associations with the symptoms of the disease.

Acknowledgements

References

1. Eskenazi B, Warner ML. Epidemiology of endometriosis. Obstet Gynecol Clin North Am 1997;24:235–258. [PubMed: 9163765]

2. Gruppo italiano per lo studio dell'endometriosi. Prevalence and anatomical distribution of endometriosis in women with selected gynecological conditions: results from a multicentric Italian study. Hum Reprod 1994;9:1158–1162. [PubMed: 7962393]

3. Sampson JA. Peritoneal endometriosis due to menstrual dissemination of endometrial tissue into the peritoneal cavity. Am J Obstet Gynecol 1927;14:422–469.

4. Meyer R. über den Stand der Frage der Adenomyositis und Adenomyome serosepithelialis und Adenomyometritis sarcomatosa. Zentrakbl Gynäko 1919;43:745–750.

5. Jones CJP, Denton J, Fazleabas AT. Morphological and glycosylation changes associated with the endometrium and ectopic lesions in a baboon model of endometriosis. Hum Reprod 2006;21:3068–3080. [PubMed: 17018533]

6. American Society for Reproductive Medicine. Revised American Society for Reproductive Medicine classification of endometriosis. Fertil Steril 1996;67:817–821.

7. Armstrong EM, More IAR, McSeveney D, Chatfield WR. Reappraisal of the ultrastructure of the human endometrial gland cell. J Obs Gyn Brit Comm 1973;80:446–460.

8. Gordon M. Cyclic changes in the fine structure of the epithelial cells of human endometrium. Int Rev Cytol 1975;42:127–172. [PubMed: 172466]

9. Verma V. Ultrastructural changes in human endometrium at different phases of the menstrual cycle and their functional significance. Gynecol Obstet Invest 1983;15:193–212. [PubMed: 6341179]

10. Cornillie FJ, Lauweryns JM, Brosens IA. Normal human endometrium—an ultrastructural survey. Gynecol Obstet Invest 1985;20:113–129. [PubMed: 4085915]

11. Dockery P, Li TC, Rogers AW, Cooke ID, Lenton EA. The ultrastructure of the glandular epithelium in the timed endometrial biopsy. Hum Reprod 1988;3:826–834. [PubMed: 3182973]

12. Bulun SE, Zeitoun KM, Takayama K, Sasano H. Estrogen biosynthesis in endometriosis: molecular basis and clinical relevance. J Mol Endocrinol 2000;25:5–42.

13. Schweppe KW. Endometriotic lesions: location, gross, histologic, and ultrastructural aspects. Prog Clin Biol Res 1990;323:33–47. [PubMed: 2406752]

14. Schweppe KW, Wynn RM. Ultrastructural changes in endometriotic implants during the menstrual cycle. Obstet Gynecol 1981;58:463–473.

15. Schweppe KW, Wynn RM, Beller FK. Ultrastructural comparison of endometriotic implants and eutopic endometrium. Am J Obstet Gynecol 1984;148:1024–1039. [PubMed: 6711624]

16. Horbelt DV, Delmore JE, Parmley TH, Roberts DK, Walker N. The nuclear channel system in endometrial adenocarcinoma exposed to medroxyprogesterone acetate. Hum Pathol 1996;27:9–14. [PubMed: 8543319]

17. Bulun SE, Cheng YH, Yin P, et al. Progesterone resistance in endometriosis: link to failure to metabolize estradiol. Mol Cell Endocrinol 2006;248:94–103. [PubMed: 16406281]

18. Ghadially, FN. Ultrastructural Pathology of the Cell and Matrix. Vol. 3. London, UK: Butterworths; 1988.

19. Ramaekers F, van Niekerk C, Poels L, et al. Use of monoclonal antibodies to keratin 7 in the differential diagnosis of adenocarcinomas. Am J Pathol 1990;136:641–655. [PubMed: 1690512]

20. Moll R, Pitz S, Levy R, Weikel W, Franke WW, Czernobilsky B. Complexity of expression of intermediate filament protein, including glial filament protein, in endometrial and ovarian adenocarcinomas. Hum Pathol 1991;22:989–1001. [PubMed: 1842387]

21. Zhao C, Bratthauer GL, Barner R, Vang R. Comparative analysis of alternative and traditional immunohistochemical markers for the distinction of ovarian sertoli cell tumour from endometrioid tumours and carcinoid tumour. Am J Surg Pathol 2007;31:255–266. [PubMed: 17255771]

22. Nakamura M, Katabuchi H, Tohya T, Fukumatsu Y, Matsuura K, Okamura H. Scanning electron microscopic and immunohistochemical studies of pelvic endometriosis. Hum Reprod 1993;8:2218–2226. [PubMed: 8150927]

23. Nakayama K, Masuzawa H, Li S-F, et al. Immunohistochemical analysis of the peritoneum adjacent to endometriotic lesions using antibodies for Ber-EP4 antigen, estrogen receptors, and progesterone receptors: implication of peritoneal metaplasia in the pathogenesis of endometriosis. Int J Gynecol Path 1994;13:348–358. [PubMed: 7814197]

24. Herrick SE, Mutsaers SE. Mesothelial progenitor cells and their potential in tissue engineering. Int J Biochem Cell Biol 2004;36:621–642. [PubMed: 15010328]

25. Czernobilsky, B.; Fox, H. Endometriosis. In: Fox, H.; Wells, M., editors. Haines and Taylor Obstetrical and Gynaecological Pathology. Vol. 5. Edinburgh, UK: Churchill Livingstone; 2003. p. 963-987.

26. Okamura H, Katabuchi H, Nitta M, Ohtake H. Structural changes and cell properties of human ovarian surface epithelium in ovarian pathophysiology. Microsc Res Tech 2006;69:469–481. [PubMed: 16718660]

27. Kerner H, Gaton E, Czernobilsky B. Unusual ovarian, tubal and pelvic mesothelial inclusions in patients with endometriosis. Histopathology 1981;5:277–283. [PubMed: 6263781]

28. Matsuura K, Ohtake H, Katabuchi H, Okamura H. Coelomic metaplasia theory of endometriosis: evidence from in viv0 studies and an in vitro experimental model. Gynecol Obstet Invest 1999;47 (suppl 1):18–22. [PubMed: 10087424]

29. Fasciani A, Bocci G, Xu J, et al. Three-dimensional in vitro culture of endometrial explants mimics the early stages of endometriosis. Fertil Steril 2003;80:1137–1143. [PubMed: 14607564]

30. Witz CA, Cho S, Centonze VE, Montoya-Rodriguez IA, Schenken RS. Time series analysis of transmesothelial invasion by endometrial stromal and epithelial cells using three-dimensional confocal microscopy. Fertil Steril 2003;79(suppl 1):770–778. [PubMed: 12620490]

31. Witz CA, Thomas MR, Montoya-Rodriguez IA, Nair AS, Centonze VE, Schenken RS. Short-term culture of peritoneum explants confirms attachment of endometrium to intact peritoneal mesothelium. Fertil Steril 2001;75:385–390. [PubMed: 11172844]

32. Zeitvogel A, Baumann R, Starzinski-Powitz A. Identification of an invasive, N-cadherin-expressing epithelial cell type in endometriosis using a new cell culture model. Am J Pathol 2001;159:1839–1852. [PubMed: 11696444]

33. Starzinski-Powitz A, Zeitvogel A, Schreiner A, Baumann R. In search of pathologic mechanisms in endometriosis: the challenge for molecular biology. Curr Mol Med 2001;1:655–664. [PubMed: 11899254]

34. Jackson, KS.; Mavrogianis, PA.; Hastings, JM.; Fazleabas, AT. Alterations in E-Cadherin (E-Cad) and Tissue Transglutaminase II (tTgaseII) during the Window of Implantation in a Baboon Model of Endometriosis (Abstract 62). Presented at the 54th Annual Meeting of the Society for Gynecological Investigation; Reno, NV. March 2007;

35. Zeitoun KM, Takayama K, Sasano H, et al. Deficient 17β-hydroxysteroid dehydrogenase type 2 expression in endometriosis: failure to metabolize 17β-estradiol. J Clin Endocrinol Metab 1998;83:4474–4480. [PubMed: 9851796]

36. Attia GR, Zeitoun K, Edwards D, Johns A, Carr BR, Bulun SE. Progesterone receptor isoform A but not B is expressed in endometriosis. J Clin Endocrinol Metab 2000;85:2897–2902. [PubMed: 10946900]

37. Noble LS, Simpson ER, Johns A, Bulun SE. Aromatase expression in endometriosis. J Clin Endocrinol Metab 1996;81:174–179. [PubMed: 8550748]

38. Zeitoun KM, Bulun SE. Aromatase: a key molecule in the pathophysiology of endometriosis and a therapeutic target. Fertil Steril 1999;72:961–969. [PubMed: 10593363]

39. Cooke PS, Buchanan DL, Lubahn DB, Cunha GR. Mechanism of estrogen action: lessons from the estrogen receptor-α knockout mouse. Biol Reprod 1998;59:470–475. [PubMed: 9716542]

40. Matsuzaki S, Murakami T, Uehara S, Canis M, Sasano H, Okamura K. Expression of estrogen receptor alpha and beta in peritoneal and ovarian endometriosis. Fertil Steril 2001;75:1198–1205. [PubMed: 11384649]

41. Nisolle M, Casanas-Roux F, Wyns Ch, De Menten Y, Mathieu PE, Donnez J. Immunohistochemical analysis of estrogen and progesterone receptors in endometrium and peritoneal endometriosis: a new quantitative method. Fertil Steril 1994;62:751–759. [PubMed: 7523199]

42. Nisolle, M.; Donnez, J. The Identification of Three Separate Diseases. New York, NY: Parthenon Publishing; 1997. Peritoneal, Ovarian and Recto-Vaginal Endometriosis.

43. Fujishita A, Nakane PK, Koji T, et al. Expression of estrogen and progesterone receptors in endometrium and peritoneal endometriosis: an immunohistochemical and in situ hybridization study. Fertil Steril 1997;67:856–864. [PubMed: 9130890]
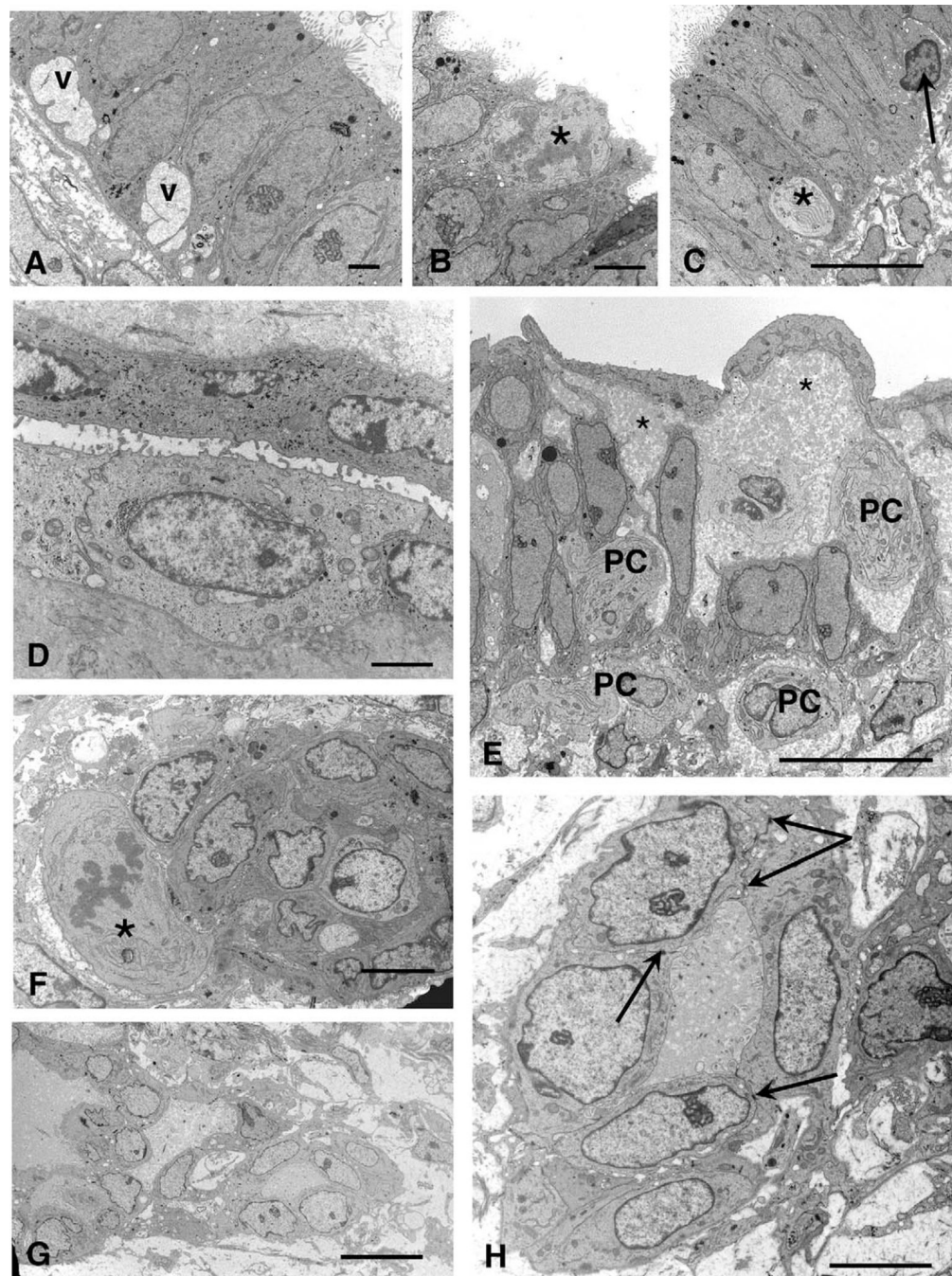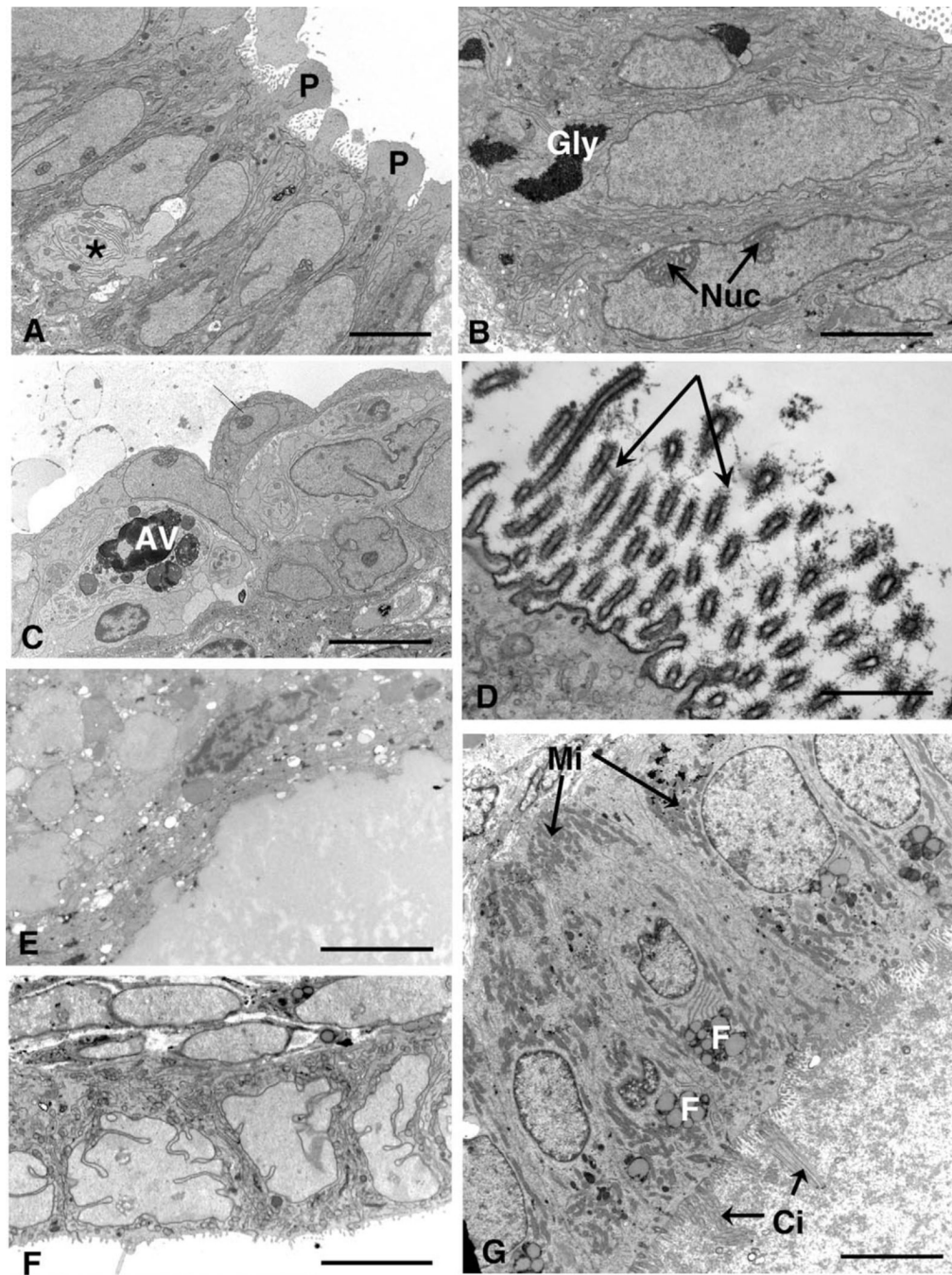
Figure 1.
A, (A–D) Day 9 (PL003): A cyst is lined by columnar cells with euchromatic nuclei and large, complex nucleoli. Large cytoplasmic basal vacuoles (v) are present in some cells. Scale bar 2 μm. B, A mitotic figure (★) can be seen in the apical area near the lumen. Scale bar 5 μm. C, Columnar epithelium closely resembling eutopic endometrium, with a profile of a pale cell (★) and intraepithelial lymphocyte (arrow). Scale bar 10 μm. D, Flattened cells from the same lesion, probably derived from mesothelium, forming a gland-like structure. Scale bar 2 μm. E, Day 15 lesion (PL002): Intercellular spaces filled are with flocculent material (★) and contain some pale cells (PCs), some of which appear to have moved into the stromal compartment.

Scale bar: 10 μm. F, (F–H) Day 17 lesion (PL005): This nest of cells has a mitotic figure (★) adjoining it. Scale bar 5 μm. G, A network of linked cells can be seen, forming tubular structures. Scale bar: 10 μm. H, Tubular structure at higher magnification showing desmosomes (arrows) joining adjacent cells. Scale bar: 5 μm.
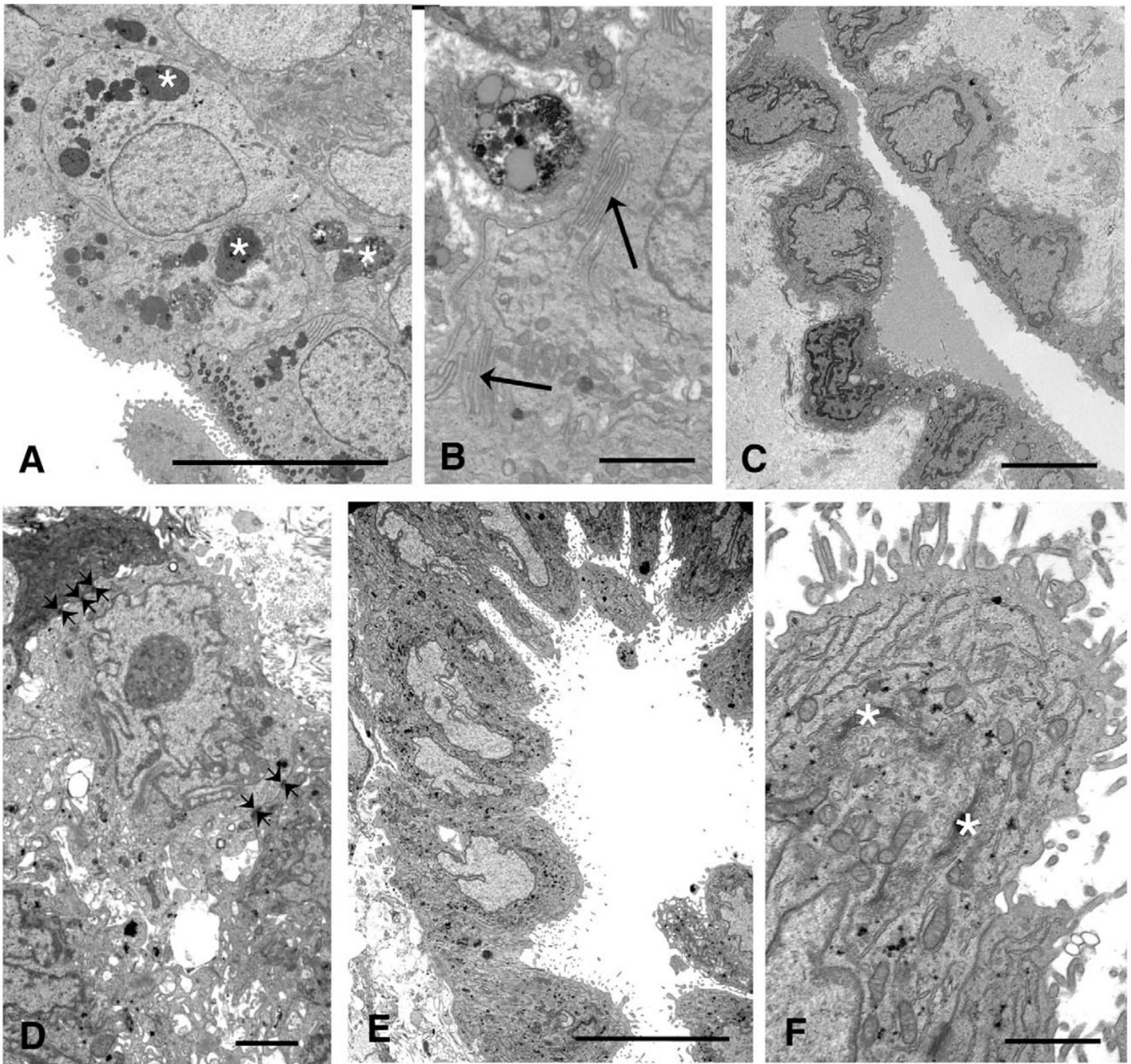
Figure 2.
A, Day 15 cyst (PL001) with well-developed pinopodes (P) on the columnar epithelial cells, between which part of a pale cell can be seen (★). Nuclei are very euchromatic and narrow cisternae of endoplasmic reticulum can be seen. B, Day 17 (PL005): Some of the glands in the peritoneal lesion contain aggregates of glycogen (Gly). Note the large nucleoli (Nuc). C, Day 15 (PL001): A cell containing large autophagic vacuoles (AV) is present between the cyst lining cells and overlies an intraepithelial lymphocyte. Pale cells can be seen in the adjoining intercellular space. Scale bars A–C: 5 μm. D, Day 17 (PL021): A prominent glycocalyx (arrows) can be seen in this part of the lining cells, with evenly spaced filaments. Scale bar: 1

μm. E, Day 21 (PL031): This lesion consisted of a large cyst lined by fatty, fibrotic cells. F, Day 17 (PL027): The cyst is lined by cuboidal cells in which nuclei are heavily incised and assume bizarre forms. G, Day 22 (PL024): A small cyst from day 22 has lining cells bearing stiff cilia (Ci), clusters of small mitochondria (Mi) basally as well as elsewhere, and fatty vesicles (F). Scale bars E–G: 5 μm.

Figure 3.
A, Day 27 (PL022): This lesion contains many heterolysosomes (★) of many different shapes
and forms. Scale bar 10 μm. B, Day 27 (PL022): Basolateral infoldings can be seen between
the cells (arrows). Scale bar 2 μm. C, Day 13 (PL006): The scalloped surface mesothelial cells
with typical heterochromatic nuclei have formed a glandular structure in this lesion. Scale bar
5 μm. D, Day 20 (PL023): This lesion contained no glands but a nest of cells with desmosomes
linking them (small arrows) was seen in the stroma. Scale bar: 2 μm. E, Day 20 (PL023): Part
of the surface mesothelium of the lesion was composed of large, tongue-like cells, dipping
down into the stroma. Scale bar 10 μm. F, Day 20 (PL023): High power of one of the tongue-
like cells (bottom left) showing abundant endoplasmic reticulum and Golgi saccules (★). Scale
bar 2 μm.
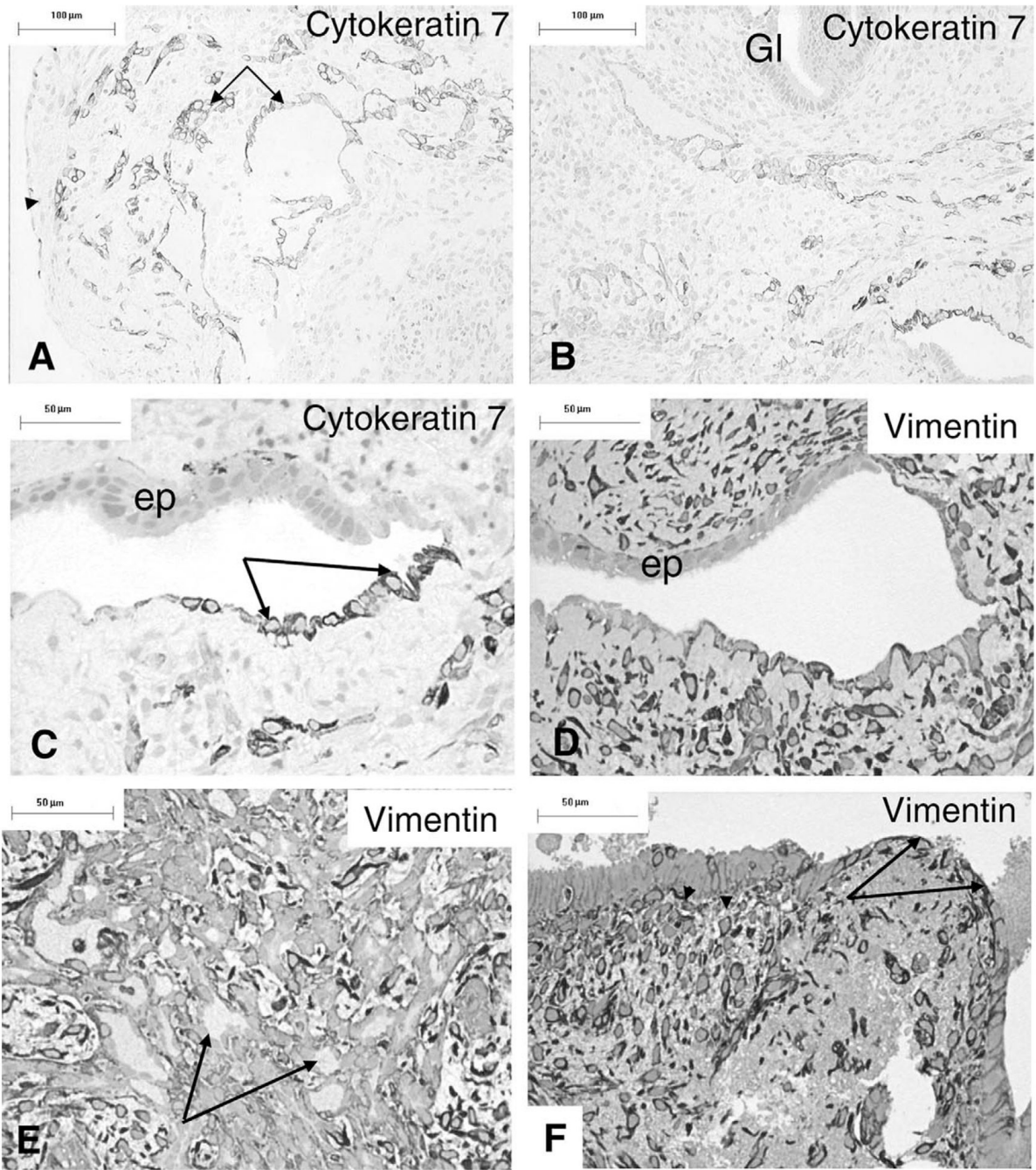
Figure 4.
Immunocytochemistry. A, Day 17 (PL005) peritoneal lesion expresses cytokeratin-7 on occasional surface cells (arrowhead) and glandular structures (arrows) in the stroma. B, A different field from the same section, showing normal glands (Gl) are unstained. C, Higher power view of the area shown bottom right in (B), with apparent epithelial transformation. The mesothelium expresses cytokeratin-7 (arrows) while the epithelium does not. D, A section of the same area but deeper in the tissue showing antivimentin staining of the mesothelial and some stromal cells; the glandular epithelium (ep) is not stained. E, The glandular structures with lumina (arrows) do not express vimentin as strongly as the surrounding stromal cells. F, An area from the surface of a day 15 cystic gland (PL001) showing thin, vimentin-positive

mesothelial cells on the surface (arrows) and in the stroma, as well as some occasional intraepithelial cells (arrowheads). Scale bars A,B: 100 μm, C–F: 50 μm.

Table 1

Details of the Ectopic Biopsies From Women With Endometriosis

Spec Number	Stage of Disease	Day of Cycle	Ultrastructural Examination
PL016	III	5	+(Meso only)
PL003	II	9	+
PL006	IV	13	+(Meso only)
PL001	I	15	+
PL017	III	15	+
PL005	III	17	+
PL027	III	17	+
PL021	I	17	+
PL023	III	20	+(Meso only)
PL028	I	21	+(Meso only)
PL031	III	21	+
PL024	III	22	+
PL026	III	24	+
PL025	IV	24	+(Meso only)
PL030	III	25	+(Meso only)
PL022	IV	27	+
PL029	III	29	+(Meso only)

Abbreviation: Meso only, mesothelium only in lesion.

Table 2

Characteristics of Glandular Cells in Ectopic Lesions

Day of Cycle	9	15	15	17	17	17	21	22	24	27
PL Number	003	001	017	005	021	027	031	024	026	022
Cell shape	Columnar	Columnar	Cuboidal	Columnar	Cuboidal	Cuboidal	Flat	Columnar/cuboidal	Cuboidal	Cuboidal
Nuclei (Het/euch)	Euch	Euch	Euch	Euch	Euch	Euch	Het	Euch	Euch/het	Euch
Nuclei (Incised)	–	–	+	–	+	+++	–	–	–/+	–
Mitos	++	++	+++	++	+	++	+	+++	++	++
ER	+	++	+	+	+	+	±	++	+	+
Golgi	+	++	+	++	++	+	±	+	±	+
Glycogen	±	±	±	++	±	±	±	+	±	±
Secret. drops	++	+	+	+	++	+	++Fatty	+++Fatty	+	+++
Microvilli	+	+	+	+	+	+Short	±	+	+short	+short
Pinopods	–	+	+	–	–	–	–	–	–	–
Cilia	–	±	±	–	–	+	–	++Straight	+	+
Pale cells	+	++	–	++	+	–	–	–	–	–
Nests	–	+	+	++	+	–	–	–	–	–
Special features	Basal vacs	Heterolysos		New glands	Glycol- calyx	Intracyt vacuole	Degenerate	Clumped cilia		Heterolysosomes

Abbreviations: ER, endoplasmic reticulum; Euch, euchromatic; het, heterochromatic; heterolysos, heterolysosomes; vacs, vacuoles.

Table 3

Characteristics of Mesothelial Cells in Ectopic Lesions

Day of Cycle	5	13	20	21	24	25	29
PL Number	016	006	023	028	025	030	029
Cell shape	Flat	Scalloped	Cuboid/tongue-like	Scalloped	Flat	Flat	Flat/tongue-like
Nuclei (Het/euch)	Het	Het	Het/euch	Het	Het	Het	Het
Nuclei (Incised)	−	+	+	−	−	+	−
Mitos	+	++	+	+	+	+	+
ER	+	++	++	+	+	+	+
Golgi	±	+	+	±	±	±	±
Glycogen	±	+	+	±	+	±	+
Secret. drops	+Fatty	+	+	±	+Fatty	±	±
Microvilli	−	Short	+	−	Blebby	Sparse	+
Pinopodes	−	−	−	−	−	−	+
Cilia	−	−	−	−	−	−	−
Pale cells	−	−	−	−	−	−	−
Nests	−	−	+	−	−	−	−
Special features		Invaginations +secretions				Necrotic area	Flocculent material in intercellular space

Abbreviations: ER:, Euch, euchromatic; Het: heterochromatic.